Electric Power Systems Research 179 (2020) 106076

Contents lists available at ScienceDirect

Electric Power Systems Research

journal homepage: www.elsevier.com/locate/epsr

An MIP-based model for the deployment of fault indicators and sectionalizing switches in distribution networks

Longjun Wang[a], Jian Lin[a], Guowei Liu[b], Gang Wang[a,*], Qing Zhong[a], Yuming Zhao[b]

[a] School of Electric Power Engineering, South China University of Technology, Guangzhou 510640, China
[b] Shenzhen Power Supply Co., Ltd., Shenzhen 518001, China

ARTICLE INFO

Keywords:
Distribution system reliability
Optimal allocation
Position matrix
Mixed-integer programming
Fault indicator
Sectionalizing switch

ABSTRACT

Fault indicators (FIs) and sectionalizing switches (SSs) are of great importance in distribution automation for reliability enhancement and efficiency improvement. However, their types and locations have great effects on the resulting service quality. This paper intends to develop a model for the optimal simultaneous allocation of FIs and SSs in a complex distribution network based on reliability and cost-benefit analyses. Three position matrices are obtained by preprocessing the topology of distribution networks to enable the establishment of the proposed model. Furthermore, a quantification method for the customer interruption duration under different contingencies is constructed to achieve a more precise and practical reliability evaluation. The resultant optimization problem is formulated as a mixed-integer linear programming that can obtain the global optimal solution in a finite number of iterations. An IEEE 33-bus network and a real urban distribution system are used to verify the effectiveness and efficiency of this model. The obtained outcomes show that simultaneously considering the placement of FIs and SSs can expedite the fault location and isolation processes, reduce the overall costs of the system and improve the service reliability.

1. Introduction

Nowadays customers have increasing demands for a higher-quality and more reliable power supply. The distribution network, which is at the terminal of an electrical power system, has a significant impact on end-users. It is estimated that approximately 70% of customer interruptions are caused by distribution system failures [1]. Hence, it is extremely urgent for electric utilities to promote the efficiency and improve the reliability of distribution networks [2]. Distribution automation systems (DASs) can accelerate fault location and isolation procedures, thereby reducing the customer interruption duration. Fault indicators (FIs) and sectionalizing switches (SSs), which comprise remote-controlled switches (RCSs) and manual switches (MSs), are prevalent apparatuses in DASs for reliability enhancement. However, it is neither necessary nor affordable to apply FIs and SSs in all candidate locations. In this regard, it is worthwhile to conduct a cost-benefit analysis to economically justify the deployment of FIs and SSs.

The importance of reducing the fault location time becomes more meaningful when considering that it takes approximately 25% of the total service restoration time associated with the manual restoration of customers [3,4]. FI is a fault current detection device. When an FI senses an inrush of fault current, it will trip and transmit the information to the outage management system [5]. Operators can identify the location of the failure more quickly from the indication of FIs. In addition, some customers are left without power during the period of fault location and repair, which decreases the service quality of the overall system. SSs can isolate the failure and restore power to some customers by switching actions, thus reducing the outage time.

The problem of placing FIs and SSs in distribution systems is generally formulated as a combinatorial optimization problem. It is seen that heuristic algorithms, including the ant colony algorithm [6], genetic algorithm (GA) [7], simulated annealing algorithm [8] and memetic algorithm [9], have been extensively used to handle the SS allocation problem. The authors in Ref. [10] proposed a method to enhance the distribution system restoration capability by upgrading the MSs to RCSs and using a greedy algorithm. In Ref. [11], an immune algorithm (IA) was utilized to derive the optimal placement of SSs by minimizing the total cost of customer service outage and the investment cost of SSs. The model described in Ref. [12] presents a multiobjective optimization approach for SS placement based on the particle swarm optimization (PSO) method. In addition, several authors address the problem with classical optimization methods. The authors in Ref. [13]. presented a two-stage decomposition approach that divides the RCS placement problem into several independent subspaces and attains the

* Corresponding author.
E-mail address: wangg@scut.edu.cn (G. Wang).

https://doi.org/10.1016/j.epsr.2019.106076
Received 14 November 2018; Received in revised form 22 June 2019; Accepted 14 October 2019
Available online 05 November 2019
0378-7796/ © 2019 Elsevier B.V. All rights reserved.

Nomenclature

n, N_n	Index and set of load points
j', j, l	Indices of branches
N_l	Set of branches
t, N_t	Index and set of years
f, N_f	Index and set of feeders
$\mathcal{E}$, M	Sufficiently small/large positive constant
d	Annual discount rate
q	Annual growth rate of load
$P_{f,n}$	Average demand of load point n in feeder f
I^{FI}, I^{RCS}, I^{MS}	Investment costs of FI, RCS, and MS, respectively
M^{FI}, M^{RCS}, M^{MS}	Maintenance costs of FI, RCS, and MS, respectively
t^{auto}	Restoration time associated with automatic switching
t^{rep}	Repair time of a faulted branch
t_f^{pre}	Preparation time for repair crews to arrive at faulted feeder f
$t_f^{\max}$	Maximum time required for fault location of faulted feeder f
V_{patrol}	Average patrolling speed of repair crews
$Le_{f,l}$	Length of branch l in feeder f
$\lambda_{f,l}$	Failure rate of branch l in feeder f
e_{unit}	Unit interruption cost
$X_{f,l}^{RCS}$, $X_{f,l}^{MS}$, $X_{f,l}^{FI}$	Binary investment decision variable, which is equal to 1 if an RCS, MS, or FI is installed on branch l in feeder f, and 0 otherwise
C^{cap}	Equipment capital cost
C^{main}	Maintenance cost of equipment
C^{out}	Expected outage cost to customers
$b_{f,j,l}$	Integer variable indicating the number of RCSs and FIs between faulted branch l and non-faulted branch j in feeder f
$L_{f,j,l}$	Binary variable indicating whether branch j is involved in the faulted zone when there is a fault in branch l in feeder f
$t_{f,l}^{loc}$	Precise fault location time when there is a fault at branch l in feeder f
$v_{f,n,l}^{RCS}$, $v_{f,n,l}^{MS}$	Binary variable indicating whether there exist RCSs, or MSs between load point n and branch l in feeder f
$t_{f,n,l}$	Interruption duration of load point n when there is a fault in branch l in feeder f
$t_{f,n,l}^{RCS}$, $t_{f,n,l}^{MS}$	Interruption duration of load point n using an RCS, or MS to isolate faulted branch l in feeder f
$C_{f,n,l}$, $G_{f,n,l}$, $t_{f,n,l}^{RCS,add}$, $t_{f,n,l}^{MS,add}$	Ancillary variables used to compute $t_{f,n,l}$

best solution in each subspace. The studies in Refs. [14,15]. developed mixed-integer programming (MIP) for the optimal placement of SSs. Moreover, several efforts have been devoted to formulating the SS placement problem as an MIP and consider the switch malfunction probability [16,17].

As an advance in fault detection technology, FIs have attracted the attention of an increasing number of researchers [18–20] present good examples of solving the FI deployment problem using the GA. In Ref. [21], the optimal FI placement via PSO is investigated while considering the impact of existing protection and control devices on the customer restoration time. In Refs. [5] and [22], the IA is adopted to optimally place FIs and achieve a tradeoff between the customer interruption cost and FI-related costs. Additionally, a relationship matrix between possible fault locations and line currents is derived based on FIs in Ref. [23] to determine the faulted line-section locations automatically and quickly. More specifically, the authors of Ref. [24] determined the optimal placement of FIs using the MIP formulation and took a pragmatic fault location procedure into account.

To the best of the authors' knowledge, little attention has been paid to the placement of FIs with joint consideration of SSs. Both RCSs and FIs act as fault detectors, and hence, a more accurate fault location time can be achieved by considering them together. An optimal placement of FIs and SSs via a GA was presented in Ref. [25] to improve the reliability of distribution networks. In Ref. [25], authors did not take into account the fault location time, and RCSs were just considered in the fault isolation procedure. The primary disadvantages of the heuristic algorithm are the excessive run time and lack of reproducibility in repeated runs [24]. The authors in Ref. [26] proposed an MIP-based model to simultaneously place FIs and SSs. However, the failure recovery analysis in Ref. [26] is based on the premise that the end of each feeder has a reserve connection, which is obviously not in accordance with the practical situation of networks. Moreover, the establishment of the model in Ref. [26] depends on the branch and location numbering method, which is applicable to only specific networks. The numbering method is unable to determine the upstream and downstream relationship between customers and a fault in a network with multiple lateral branches, and thus, it is not applicable to radial distribution systems.

Considering the limitations of the above models, this paper proposes a new methodology for the deployment of FIs and SSs in complex distribution systems. The main contributions are as follows: (1) Three position matrices are obtained by preprocessing the topology of the distribution network. The available positions of FIs and SSs in networks for reliability evaluation are characterized in advance by the matrices. With them, the proposed model can be established and handle the placement of FIs and SSs in complex distribution networks that have

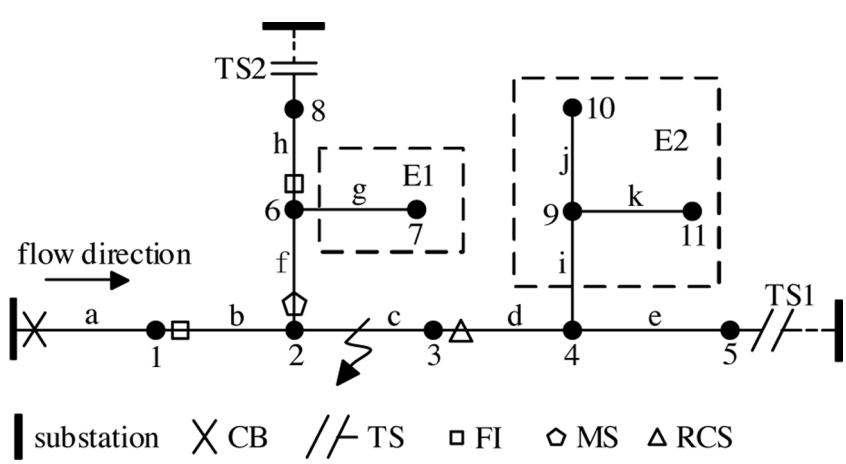

Fig. 1. A representative feeder to describe the problem statement.

multiple lateral branches. (2) As FIs and RCSs have the function of fault detection, the practical fault location process is considered in this paper. Additionally, the customer interruption duration under different contingencies is concretely discussed to obtain more precise results. (3) By utilizing linearization techniques, the FI and SS placement problem is mathematically formulated as an MIP model in this paper. Compared with a heuristic algorithm, the global optimal solution can be obtained in a finite number of iterations.

The remainder of this paper is organized as follows. The problem statement is put forward in Section 2. Section 3 describes the proposed optimal placement model of FIs and SSs in detail. Two case studies with discussions are presented in Section 4. Finally, conclusions are drawn in Section 5.

2. Problem statement

Generally, a complex radial distribution network is a network with multiple lateral branches. In this paper the lateral branch is considered to have the same structure as the simple radial network (except for the tie branch and switch). Taking the distribution network in Fig. 1 as an example, there are two lateral branches that are located in the dashed line boxes. The positive direction of each branch is the same as the direction of power flow. Electric utilities usually equip a modest number of FIs and SSs on overhead lines due to the limited investment and numerous branches in distribution networks [27]. Generally, in practical engineering, only one switch is installed on a branch, and it is configured at the beginning of the branch. Therefore, for the sake of simplicity, this paper assumes that the FIs, RCSs, and MSs are all installed at the beginning of each branch, and their malfunction probability is ignored. Tie switches (TSs), which are located at the ends of feeders, can connect neighboring feeders for better supply reliability and are considered as automatic switches.

Supposing a fault occurs in branch c, first, the circuit breaker (CB) trips and all load points are de-energized. Meanwhile, the FI on branch b trips, but the FI on branch h and the FI embedded in the RCS on branch d do not act. Therefore, the operators can deduce that the fault is either on branch b, c, f, or g. Next, the loads downstream of the fault, including load points (LPs) 4–5 and 9–11, can be restored promptly by opening the RCS on branch d and closing TS1. Then, repair crews are arranged to patrol the fault suspicious zone. After identifying the fault located on branch c, service is restored to LPs 6–8 by opening the MS on branch f and closing TS2. LPs 1–3 would be kept interrupted until the fault is repaired.

3. MIP-based deployment model

3.1. Definitions of three position matrices

3.1.1. FI and RCS position matrix

From the analysis above, it is determined that whether the non-faulted branch is involved in the faulted zone depends on whether there exist FIs or RCSs between the terminals of the non-faulted branch and the faulted branch. Therefore, an FI and RCS position matrix (FRPM) $\boldsymbol{W}$ is established in this paper to describe the pathway between the terminals of the non-faulted branch and the faulted branch. The elements in $\boldsymbol{W}$ are '0' and '1'. $w_{f,j',j,l} = 1$ represents branch j' being passed between the terminals of non-faulted branch j and faulted branch l at feeder f. For example, if a fault occurs in branch c in Fig. 1, $\boldsymbol{W_c}$ is expressed as follows:

$$\begin{array}{c} \\ a \\ b \\ c \\ d \\ e \\ f \\ g \\ h \\ i \\ j \\ k \end{array} \begin{array}{c} \begin{array}{ccccccccccc} a & b & c & d & e & f & g & h & i & j & k \end{array} \\ \begin{bmatrix} 0 & 1 & 1 & 0 & 0 & 0 & 0 & 0 & 0 & 0 & 0 \\ 0 & 0 & 1 & 0 & 0 & 0 & 0 & 0 & 0 & 0 & 0 \\ 0 & 0 & 0 & 0 & 0 & 0 & 0 & 0 & 0 & 0 & 0 \\ 0 & 0 & 0 & 1 & 0 & 0 & 0 & 0 & 0 & 0 & 0 \\ 0 & 0 & 0 & 1 & 1 & 0 & 0 & 0 & 0 & 0 & 0 \\ 0 & 0 & 1 & 0 & 0 & 1 & 0 & 0 & 0 & 0 & 0 \\ 0 & 0 & 1 & 0 & 0 & 1 & 1 & 0 & 0 & 0 & 0 \\ 0 & 0 & 1 & 0 & 0 & 1 & 0 & 1 & 0 & 0 & 0 \\ 0 & 0 & 0 & 1 & 0 & 0 & 0 & 0 & 1 & 0 & 0 \\ 0 & 0 & 0 & 1 & 0 & 0 & 0 & 0 & 1 & 1 & 0 \\ 0 & 0 & 0 & 1 & 0 & 0 & 0 & 0 & 1 & 0 & 1 \end{bmatrix} \end{array}$$

The row and column numbers of $\boldsymbol{W_c}$ are the numbers of branches. The first row of the matrix means that the branches between the terminals of branch a and faulted branch c include branches b and c. In other words, when a fault occurs in branch c, branch a could be excluded from the faulted zone as long as there is an FI or an RCS installed in branch b or c. Note that $\boldsymbol{W_c}$ is simply part of $\boldsymbol{W}$; similar matrices can be formed when the failure occurs in other branches.

3.1.2. RCS and MS position matrix

In Fig. 1, if a fault occurs in branch c, LPs 9–11 remain interrupted even if there is a switch on branch i to isolate the fault, as there is no reserve connection to restore power for LPs 9–11. In light of the above situation, an RCS and MS position matrix (RMPM) $\boldsymbol{H}$ is proposed in this paper to describe the pathway between the load point and the terminal of the faulted branch. To make our method applicable for distribution systems, the lateral branch is merged as one equivalent load point in the process of obtaining the RMPM. For example, lateral branches E1 and E2 in Fig. 1 are equivalent to LP 6 and 4, respectively. Hence, for load points located on the lateral branch, the RMPM is the pathway between the equivalent load point and the terminal of the faulted branch. The elements in $\boldsymbol{H}$ are '0' and '1'. $h_{f,j,n,l} = 1$ represents that branch j is passed through between load point n and the terminal of faulted branch l at feeder f. Supposing that a fault occurs in branch c in Fig. 1, $\boldsymbol{H_c}$ is expressed as follows:

$$\begin{array}{c} \\ 1 \\ 2 \\ 3 \\ 4 \\ 5 \\ 6 \\ 7 \\ 8 \\ 9 \\ 10 \\ 11 \end{array} \begin{array}{c} \begin{array}{ccccccccccc} a & b & c & d & e & f & g & h & i & j & k \end{array} \\ \begin{bmatrix} 0 & 1 & 1 & 0 & 0 & 0 & 0 & 0 & 0 & 0 & 0 \\ 0 & 0 & 1 & 0 & 0 & 0 & 0 & 0 & 0 & 0 & 0 \\ 0 & 0 & 0 & 0 & 0 & 0 & 0 & 0 & 0 & 0 & 0 \\ 0 & 0 & 0 & 1 & 0 & 0 & 0 & 0 & 0 & 0 & 0 \\ 0 & 0 & 0 & 1 & 1 & 0 & 0 & 0 & 0 & 0 & 0 \\ 0 & 0 & 1 & 0 & 0 & 1 & 0 & 0 & 0 & 0 & 0 \\ 0 & 0 & 1 & 0 & 0 & 1 & 0 & 0 & 0 & 0 & 0 \\ 0 & 0 & 1 & 0 & 0 & 1 & 0 & 1 & 0 & 0 & 0 \\ 0 & 0 & 0 & 1 & 0 & 0 & 0 & 0 & 0 & 0 & 0 \\ 0 & 0 & 0 & 1 & 0 & 0 & 0 & 0 & 0 & 0 & 0 \\ 0 & 0 & 0 & 1 & 0 & 0 & 0 & 0 & 0 & 0 & 0 \end{bmatrix} \end{array}$$

The row and column numbers of $\boldsymbol{H_c}$ correspond to the load point number and the branch number, respectively. The first row of the matrix means the branches between LP1 and the terminal of faulted branch c, including branches b and c. $\boldsymbol{H_c}$ is simply part of $\boldsymbol{H}$; similar matrices can be formed when a failure occurs in other branches. It should be noted that when a failure occurs in the lateral branch, the load points on the main section of this lateral branch no longer perform equivalent processing, but the sub-lateral branch is still needed for equivalence. For example, with a fault occurring in branch j, LPs 9–10 have no need for equivalence, but LP11 must be equivalent to LP9.

3.1.3. Customer position matrix

The customer position matrix (CPM) $\boldsymbol{D}$ indicates the relative position between the customer and the faulted branch as well as whether there is a reserve connection to supply power for the interrupted customer. When a fault occurs in a distribution network, the customers can be classified into 3 types: (1) upstream of the faulted branch; (2) downstream of the faulted branch with a reserve connection to supply

power for the customer; and (3) downstream of the faulted branch without a reserve connection to supply power for the customer. The elements in $\boldsymbol{D}$ are '−1,' '1,' and '0'. $d_{f,n,l} = -1, 1, 0$ represents the type of load point n, which is type 1, 2 or 3, respectively, when a fault occurs in branch l at feeder f. CPM $\boldsymbol{D}$ in Fig. 1 is built and expressed as follows:

$$\begin{array}{c} \\ a \\ b \\ c \\ d \\ e \\ f \\ g \\ h \\ i \\ j \\ k \end{array} \begin{array}{c} \begin{array}{ccccccccccc} 1 & 2 & 3 & 4 & 5 & 6 & 7 & 8 & 9 & 10 & 11 \end{array} \\ \begin{bmatrix} 1 & 1 & 1 & 1 & 1 & 1 & 1 & 1 & 1 & 1 & 1 \\ -1 & 1 & 1 & 1 & 1 & 1 & 1 & 1 & 1 & 1 & 1 \\ -1 & -1 & 1 & 1 & 1 & -1 & -1 & -1 & 1 & 1 & 1 \\ -1 & -1 & -1 & 1 & 1 & -1 & -1 & -1 & 1 & 1 & 1 \\ -1 & -1 & -1 & -1 & 1 & -1 & -1 & -1 & -1 & -1 & -1 \\ -1 & -1 & -1 & -1 & -1 & 1 & 1 & 1 & -1 & -1 & -1 \\ -1 & -1 & -1 & -1 & -1 & -1 & 0 & -1 & -1 & -1 & -1 \\ -1 & -1 & -1 & -1 & -1 & -1 & -1 & 1 & -1 & -1 & -1 \\ -1 & -1 & -1 & -1 & -1 & -1 & -1 & -1 & 0 & 0 & 0 \\ -1 & -1 & -1 & -1 & -1 & -1 & -1 & -1 & -1 & 0 & -1 \\ -1 & -1 & -1 & -1 & -1 & -1 & -1 & -1 & -1 & -1 & 0 \end{bmatrix} \end{array}$$

The row and column numbers of $\boldsymbol{D}$ correspond to the branch number and the load point number, respectively. The 9th row of $\boldsymbol{D}$ indicates that, when a fault occurs in branch i, LPs 1–8 are located upstream of the faulted branch i and there is no reserve connection to supply power for LPs 9–11.

The FRPM concludes the pathway information of the distribution networks that can be utilized to analyze whether the non-faulted branch is involved in the faulted zone. With the RMPM and the CPM, we can determine whether the affected load points by the faulted branch can be restored through proper switching actions. Based on the above three matrices, the fault location time and customer interruption duration under N-1 contingencies are formulated and built as functions of the FI, RCS and MS locations, which are respectively described in Sections 3.4 and 3.5. The topology of a distribution network can be abstracted into a graph. Thus the shortest path algorithm and reachability analysis are applied to the generation of the above three matrices.

3.2. Decision variables

The decision variables of the optimization problem are $X_{f,l}^{RCS}$, $X_{f,l}^{MS}$, and $X_{f,l}^{FI}$. According to the formulation in Section 2, it can be concluded that FIs are used to indicate the path of the fault current, and MSs are utilized to isolate failures. Moreover, RCSs could not only remotely provide information regarding fault current pathways but also isolate the faulted area from the network. Since RCSs have the functions of fault indication and fault isolation, there is no need to allocate an FI or an MS when an RCS has been installed in the candidate location.

$$X_{f,l}^{RCS} + X_{f,l}^{MS} \le 1 \quad \forall f \in N_f, l \in N_l \tag{1}$$

$$X_{f,l}^{RCS} + X_{f,l}^{FI} \le 1 \quad \forall f \in N_f, l \in N_l \tag{2}$$

Constraint (1) indicates that no more than one SS can be installed in each candidate location. Constraint (2) assures that RCS and FI are not installed at the same location.

3.3. Objective function

To assess the overall present worth of a proposed addition if it is a viable long-term asset, it must be studied over a significant portion of its lifetime. The FI and SS deployment problem is considered long-range planning for N_t years. The objective function of this model is expressed as follows:

$$\textbf{Minimize} \;\; COST = C^{cap} + C^{main} + C^{out} \tag{3}$$

$$C^{cap} = \sum_{f \in N_f} \sum_{l \in N_l} (X_{f,l}^{FI} I^{FI} + X_{f,l}^{RCS} I^{RCS} + X_{f,l}^{MS} I^{MS}) \tag{4}$$

$$C^{main} = \sum_{t \in N_t} \sum_{f \in N_f} \sum_{l \in N_l} \frac{1}{(1+d)^t} (X_{f,l}^{FI} M^{FI} + X_{f,l}^{RCS} M^{RCS} + X_{f,l}^{MS} M^{MS}) \tag{5}$$

$$C^{out} = \sum_{t \in N_t} \sum_{f \in N_f} \sum_{l \in N_l} \sum_{n \in N_n} \frac{(1+q)^{t-1}}{(1+d)^t} \lambda_{f,l} P_{f,n} t_{f,n,l} e_{unit} \tag{6}$$

Eqs. (4)–(6) correspond to the costs of investment, maintenance and customer interruption, respectively. The effects of discount and load growth rate are considered in the planning horizon. The average load is usually used as the basis for the cost effectiveness evaluation of distribution system reliability planning [27]. Note that $P_{f,n}$ in Eq. (6) is the average load of customers such as electric vehicle charging station, residential users, and industrial facilities, which can be obtained by using their load curves. In addition, the unit interruption price can be set to different values based on the corresponding customer types. A series of approximate methods to assess customer interruption costs due to specified outage events were described in Ref. [28].

3.4. Fault location

The fault location time depends on the branches that are located in the faulted zone, and the faulted zone is identified by the FIs and RCSs. As seen from the example given in Section 2, when a fault occurs in branch c, the nonzero elements of the row a elements of $\boldsymbol{W_c}$ in column b and c; meanwhile, there is an FI on branch b. Consequently, it is concluded that branch a is located out of the faulted zone. Based on the FRPM $\boldsymbol{W}$, the fault location time can be estimated as follows:

$$b_{f,j,l} = \sum_{j' \in N_l} X_{f,j'}^{FI} w_{f,j',j,l} + \sum_{j' \in N_l} X_{f,j'}^{RCS} w_{f,j',j,l} \quad \forall f \in N_f, \forall j, l \in N_l \tag{7}$$

$$\varepsilon - \frac{1}{M} b_{f,j,l} \le L_{f,j,l} \le 1 - \frac{1}{M} b_{f,j,l} + \varepsilon \quad \forall f \in N_f, \forall j, l \in N_l \tag{8}$$

$$t_{f,l}^{loc} = \sum_{j \in N_l} \frac{Le_{f,j}}{V_{patrol}} L_{f,j,l} + t_f^{pre} \quad \forall f \in N_f, \forall l \in N_l \tag{9}$$

In Eq. (7), the number of RCSs and FIs between faulted branch l and non-faulted branch j is obtained using the FRPM. In Eq. (8), the non-faulted branch j would not be involved in the faulted zone when there exists at least one FI or RCS between the non-faulted branch j and the faulted branch l. If $L_{f,j,l} = 1$, branch j is involved in the faulted zone, and repair crews are required to confirm whether the fault is located in branch j. Obviously, the value of the fault location time is influenced by the patrolling speed and preparation time of the repair crews. The fault location time is calculated as shown in Eq. (9).

3.5. Customer interruption time

The quantification method of the customer interruption duration under 8 scenarios is analyzed as follows.

Scenario 1: the customer is upstream of the faulted branch, and there exists at least one RCS between them. The customer can be restored by opening the RCS and closing CB. At this time, the customer interruption duration is the sum of the operating time of the RCS and the operating time of the CB.

Scenario 2: the customer is downstream of the faulted branch, and there exists at least one RCS between them; meanwhile, there is a reserve connection to restore power to the customer. At this time, the customer interruption duration is the sum of the operating time of the RCS and the operating time of the TS.

Scenario 3: the customer is downstream of the faulted branch, and there exists at least one RCS between them, but there is no reserve connection to restore power to the customer. At this time, the customer interruption duration is the sum of the fault location time and the fault repair time.

Scenario 4: the customer is upstream of the faulted branch and there

exists at least one MS between them without an RCS. The customer can be restored by opening the MS and closing the CB after the fault is located. At this time, the customer interruption duration is the sum of the fault location time and the operating time of the CB.

Scenario 5: the customer is downstream of the faulted branch and there exists at least one MS between them without an RCS; meanwhile, there is a reserve connection to restore power to the customer. At this time, the customer interruption duration is the sum of the fault location time and the operating time of the TS.

Scenario 6: the customer is downstream of the faulted branch and there exists at least one MS between them without an RCS, but there is no reserve connection to restore power to the customer. At this time, the customer interruption duration is the sum of the fault location time and the fault repair time.

Scenario 7/8: the customer is upstream/downstream of the faulted branch and there is neither an RCS nor an MS between them. At this time, the customer interruption duration is the sum of the fault location time and the fault repair time.

In Fig. 1, when a fault occurs in branch c, the nonzero elements of the 1th row elements of $\boldsymbol{H_c}$ in column b and c; however, there is no SS on branch b or branch c. Thus, it is concluded that there is neither an RCS nor an MS between LP1 and faulted branch c. Based on RMPM $\boldsymbol{H}$, the relationships among $X_{f,j}^{RCS}$, $X_{f,j}^{MS}$, $v_{f,n,l}^{RCS}$, and $v_{f,n,l}^{MS}$, can be expressed as:

$$\frac{\sum_{j\in N_l} X_{f,j}^{RCS} h_{f,j,n,l}}{M} \le v_{f,n,l}^{RCS} \le \sum_{j\in N_l} X_{f,j}^{RCS} h_{f,j,n,l} \quad \forall f\in N_f, \forall l\in N_l, \forall n\in N_n \tag{10}$$

$$\frac{(\sum_{j\in N_l} X_{f,j}^{MS} h_{f,j,n,l})(1-v_{f,n,l}^{RCS})}{M} \le v_{f,n,l}^{MS} \le (\sum_{j\in N_l} X_{f,j}^{MS} h_{f,j,n,l}) \times (1 - v_{f,n,l}^{RCS}) \quad \forall f\in N_f, \forall l\in N_l, \forall n\in N_n \tag{11}$$

Constraint (10) ensures that $v_{f,n,l}^{RCS} = 1$ when there exists at least one RCS between load point n and faulted branch l; otherwise $v_{f,n,l}^{RCS} = 0$. In Eq. (11), when variable $v_{f,n,l}^{RCS} = 1$, the value of $v_{f,n,l}^{MS}$ is 0 whether or not there exist MSs between load point n and faulted branch l. Furthermore, Constraint (11) can be linearized as follows:

$$v_{f,n,l}^{MS} - \sum_{j\in N_l} X_{f,j}^{MS} h_{f,j,n,l} \le M \times v_{f,n,l}^{RCS} \quad \forall f\in N_f, \forall l\in N_l, \forall n\in N_n \tag{12}$$

$$v_{f,n,l}^{MS} - \frac{\sum_{j\in N_l} X_{f,j}^{MS} h_{f,j,n,l}}{M} \ge -M \times v_{f,n,l}^{RCS} \quad \forall f\in N_f, \forall l\in N_l, \forall n\in N_n \tag{13}$$

$$-M \times (1-v_{f,n,l}^{RCS}) \le v_{f,n,l}^{MS} \le M \times (1-v_{f,n,l}^{RCS}) \quad \forall f\in N_f, \forall l\in N_l, \forall n\in N_n \tag{14}$$

Additionally, CPM $\boldsymbol{D}$ indicates the relative position between the customer and the faulted branch. Thus, the customer interruption duration in the 8 scenarios above can be expressed as follows by combining the CPM $\boldsymbol{D}$.

$$t_{f,n,l} = (t_{f,l}^{loc} + t^{rep})(1-v_{f,n,l}^{RCS})(1-v_{f,n,l}^{MS}) + t_{f,n,l}^{RCS} v_{f,n,l}^{RCS} + t_{f,n,l}^{MS}(1-v_{f,n,l}^{RCS}) v_{f,n,l}^{MS} \quad \forall f\in N_f, \forall l\in N_l, \forall n\in N_n \tag{15}$$

$$t_{f,n,l}^{RCS} = \begin{cases} 2t^{auto}, & d_{f,n,l} = -1 \\ 2t^{auto}, & d_{f,n,l} = 1 \\ t_{f,l}^{loc} + t^{rep}, & d_{f,n,l} = 0 \end{cases} \quad \forall f\in N_f, \forall l\in N_l, \forall n\in N_n \tag{16}$$

$$t_{f,n,l}^{MS} = \begin{cases} t_{f,l}^{loc} + t^{auto}, & d_{f,n,l} = -1 \\ t_{f,l}^{loc} + t^{auto}, & d_{f,n,l} = 1 \\ t_{f,l}^{loc} + t^{rep}, & d_{f,n,l} = 0 \end{cases} \quad \forall f\in N_f, \forall l\in N_l, \forall n\in N_n \tag{17}$$

Eq. (16) describes the customer interruption duration corresponding to scenarios 1–3, and Eq. (17) corresponds to scenarios 4–6. When there is neither an RCS nor an MS between the customers and the fault, i.e., $v_{f,n,l}^{MS} = v_{f,n,l}^{RCS} = 0$, it can be determined from Eq. (15) that the customer interruption duration is equal to $t_{f,l}^{loc} + t^{rep}$, corresponding to scenarios 7–8.

Eq. (15) is a complex nonlinear expression that can be linearized as follows:

$$t_f^{max} = \sum_{l\in N_l} \frac{Le_{f,l}}{V_{patrol}} + t_f^{pre} \quad \forall f\in N_f \tag{18}$$

$$C_{f,n,l} = t_{f,l}^{loc} v_{f,n,l}^{RCS} \quad \forall f\in N_f, \forall l\in N_l, \forall n\in N_n \tag{19}$$

$$0 \le C_{f,n,l} \le t_f^{max} v_{f,n,l}^{RCS} \quad \forall f\in N_f, \forall l\in N_l, \forall n\in N_n \tag{20}$$

$$t_{f,l}^{loc} - t_f^{max}(1-v_{f,n,l}^{RCS}) \le C_{f,n,l} \le t_{f,l}^{loc} \quad \forall f\in N_f, \forall l\in N_l, \forall n\in N_n \tag{21}$$

$$G_{f,n,l} = t_{f,l}^{loc} v_{f,n,l}^{MS} \quad \forall f\in N_f, \forall l\in N_l, \forall n\in N_n \tag{22}$$

$$0 \le G_{f,n,l} \le t_f^{max} v_{f,n,l}^{MS} \quad \forall f\in N_f, \forall l\in N_l, \forall n\in N_n \tag{23}$$

$$t_{f,l}^{loc} - t_f^{max}(1-v_{f,n,l}^{MS}) \le G_{f,n,l} \le t_{f,l}^{loc} \quad \forall f\in N_f, \forall l\in N_l, \forall n\in N_n \tag{24}$$

$$t_{f,n,l}^{RCS,add} = t_{f,n,l}^{RCS} v_{f,n,l}^{RCS} \quad \forall f\in N_f, \forall l\in N_l, \forall n\in N_n \tag{25}$$

$$t_{f,n,l}^{RCS,add} = \begin{cases} 2t^{auto} v_{f,n,l}^{RCS}, & d_{f,n,l} = -1 \\ 2t^{auto} v_{f,n,l}^{RCS}, & d_{f,n,l} = 1 \\ t_{f,l}^{loc} v_{f,n,l}^{RCS} + t^{rep} v_{f,n,l}^{RCS}, & d_{f,n,l} = 0 \end{cases} \quad \forall f\in N_f, \forall l\in N_l, \forall n\in N_n \tag{26}$$

$$t_{f,n,l}^{MS,add} = t_{f,l}^{MS} v_{f,n,l}^{MS} \quad \forall f\in N_f, \forall l\in N_l, \forall n\in N_n \tag{27}$$

$$t_{f,n,l}^{MS,add} = \begin{cases} t_{f,l}^{loc} v_{f,n,l}^{MS} + t^{auto} v_{f,n,l}^{MS}, & d_{f,n,l} = -1 \\ t_{f,l}^{loc} v_{f,n,l}^{MS} + t^{auto} v_{f,n,l}^{MS}, & d_{f,n,l} = 1 \\ t_{f,l}^{loc} v_{f,n,l}^{MS} + t^{rep} v_{f,n,l}^{MS}, & d_{f,n,l} = 0 \end{cases} \quad \forall f\in N_f, \forall l\in N_l, \forall n\in N_n \tag{28}$$

$$t_{f,n,l} = t_{f,n,l}^{RCS,add} + t_{f,n,l}^{MS,add} + t^{rep}(1-v_{f,n,l}^{RCS} - v_{f,n,l}^{MS}) + t_{f,l}^{loc} - G_{f,n,l} - C_{f,n,l} \quad \forall f\in N_f, \forall l\in N_l, \forall n\in N_n \tag{29}$$

Eq. (18) provides the maximum time required for the fault location of feeder f. $C_{f,n,l}$, $G_{f,n,l}$, $t_{f,n,l}^{RCS,add}$, $t_{f,n,l}^{MS,add}$ are introduced as ancillary variables. Note that both $C_{f,n,l}$ and $G_{f,n,l}$ include the product of a binary variable and a real variable; thus, they can be converted into inequality constraints (20)–(21) and (23)–(24), respectively. Combined with $v_{f,n,l}^{RCS}$ and $v_{f,n,l}^{MS}$ Eqs. (16) and (17) are adapted into the forms of Eqs. (26) and (28), respectively. Eq. (29) is the final expression of the customer interruption duration.

4. Case studies

The proposed model has been coded in the Python environment and solved using the MIP solver CPLEX 12.6 [29] on a 3.4-GHz processor with 8 GB of RAM, and the optimal gap of CPLEX is set to 0%. The most commonly used reliability indices, including the system average interruption duration index (SAIDI) and average energy not supply (AENS) [30], are applied to quantify system reliability.

4.1. IEEE 33-bus

The test network comprising 32 load points [31] is depicted in Fig. 2. Additionally, to illustrate the advantage of the presented model, we assume that the system is connected to two interconnected radial networks. The two TSs are connected to node 17 and 32, respectively.

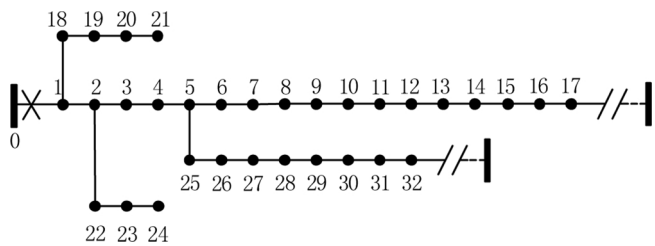

Fig. 2. Modified IEEE 33-bus network.

Table 1
Other required data.

Parameter	Value	Parameter	Value
t^{auto} (min)	5	q	0.011
t^{rep} (min)	120	d	0.05
t_f^{pre} (min)	25	V_{patrol} (km/h)	10

Table 2
Length of each branch.

Length (km)	Feeder branch numbers
0.75	1,2,3,4,6,10,11,18,20,22,25,26,29,31,32
1.6	5,7,8,13,14,15,17,21,23,24,28
2.8	9,12,16,19,27,30

Table 3
Simulated results of Cases I–VIII.

Case	Costs [U.S. k$]				Reliability indices		Numbers		
	C^{cap}	C^{main}	C^{out}	Total	AENS [kWh/yr.LP]	SAIDI [h/yr.LP]	FI	MS	RCS
I	0	0	1041.63	1041.63	5692.44	42.07	0	0	0
II	8.00	4.15	774.91	787.06	4234.88	31.34	0	16	0
III	21.00	10.90	393.60	425.50	2151.00	15.90	21	0	0
IV	28.20	14.64	81.58	124.42	445.84	3.60	0	0	6
V	28.80	14.95	68.05	111.80	371.87	2.91	4	12	4
VI	31.00	16.09	65.38	112.47	357.30	2.80	2	11	5
VII	37.40	19.41	70.00	126.81	382.46	2.93	21	14	2
VIII	145.70	75.62	42.34	263.66	231.41	1.63	0	0	31

Table 4
Optimal equipment locations of Case V.

Location		
FI	MS	RCS
8,15,23,29	3,6,7,8,13,14,16, 19,24,28,30,31	2,5,11,27

Table 5
Comparison between the proposed method and GA.

Case	Total cost [U.S. k $]	Reliability indices		Execution time
		AENS [kWh/yr.LP]	SAIDI [h/yr.LP]	
A	111.80	371.87	2.91	23.9 s
B	129.32	345.62	2.63	66.3 s
C	123.81	384.43	3.12	567.4 s

The capital investments of the RCS, MS, and FI are respectively assumed to be U.S. $4700, 500, and 1000. The annual maintenance costs are considered to be 5% of the capital investment for the equipment. The planning horizon is 15 years, other required data are listed in Table 1, and the above data can be found in Refs. [14,26]. The unit interruption cost is considered to be 0.6 $/kWh. In addition, the average failure rate is 0.132 occ./yr.km [11]. The length of each branch is shown in Table 2. To investigate the performance of the proposed model, 8 cases are used for comparison as follows.

Case I: The original network is not equipped with any FI or SS;

Case II: The network is equipped with only MSs;

Case III: The network is equipped with only FIs;

Case IV: The network is equipped with only RCSs;

Case V: The network is simultaneously equipped with FIs and SSs;

Case VI: The network is first equipped with SSs, and then the FI allocation in the network already equipped with SSs is conducted;

Case VII: The network is first equipped with FIs, and then the SS allocation in the network already equipped with FIs is conducted;

Case VIII: The objective function considers only the reliability cost.

The costs, reliability indices and equipment deployment results of Cases I–VIII are provided in Table 3. The optimal locations of the SSs and FIs of Case V are shown in Table 4.

According to the results shown in Table 3, the total cost of Case I is U.S. k$1041.63, which is the highest cost in all cases. In contrast, the total costs of Case V falls to U.S. k$111.8, nearly an 89.3% reduction, which shows that the FI and SS can dramatically decrease the overall costs. By comparing Cases II–IV, the RCS has the greatest impact on enhancing the system reliability, followed by FI and finally MS. This is because the MS can operate only after the fault is located, but both the RCS and FI are involved in the fault location process and speed it up. In addition, the simultaneous placement of FI and SS is better than a separate configuration. By comparing Cases V–VII, it can be determined that the reliability indices SAIDI and AENS of Cases VI are better than those of Case V. However, the equipment and maintenance costs of Case V are less than those of Case VI. Thus, the sequential placement of SSs and FIs cannot obtain the most economical solution. When the objective function does not consider equipment and maintenance costs, the number of deployed RCSs for Case VIII is 31. As a result, Case VIII has the lowest interruption cost (U.S. k$42.34) and the best reliability indices; on the other hand, it also has the maximum equipment cost.

Table 6
Equipment placement in sequential manner with different expected fault location times.

Expected fault location time [h]	Numbers			Reliability indices	
	RCS	MS	FI	AENS [kWh/yr.LP]	SAIDI [h/yr.LP]
0.45	2	14	9	426.01	3.27
0.65	2	14	9	426.01	3.27
0.9	4	12	5	364.12	2.83
1.15	4	12	4	373.52	2.95
1.35	5	11	2	358.24	2.79

Table 7
Impact of unit interruption cost on equipment placement.

e_{unit} ($/kWh)	Numbers			Total cost [U.S. k$]	Reliability indices	
	RCS	MS	FI		AENS [kWh/yr.LP]	SAIDI [h/yr.LP]
0.015	0	2	2	14.44	2159.56	16.16
0.1	2	4	2	40.96	675.65	5.24
0.6	4	12	4	111.80	371.87	2.91
1.2	6	17	4	172.25	301.75	2.27
3	8	20	6	328.69	270.26	1.99

4.1.1. Comparison with GA

Genetic algorithm is used to solve the proposed model under the

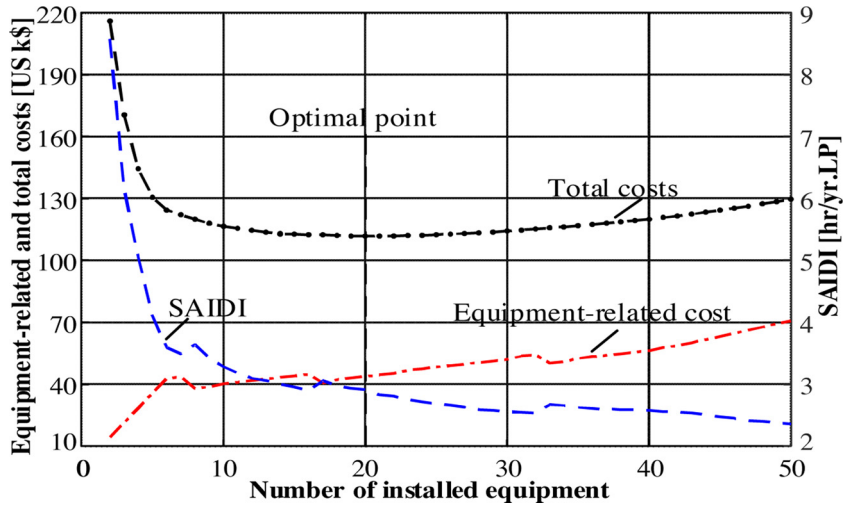

Fig. 3. Variation in the SAIDI and related costs versus the number of installed equipment.

Table 8
Simulated results of Cases I–VIII in a Finnish distribution network.

Case	Costs [U.S.k$]				Reliability indices		Numbers		
	C^{cap}	C^{main}	C^{out}	Total	AENS [kWh/yr.LP]	SAIDI [h/yr.LP]	FI	MS	RCS
I	0	0	2795.4	2795.4	59.48	1.117	0	0	0
II	34.5	17.9	1892.3	1944.7	40.26	0.771	0	69	0
III	67.0	34.8	1418.6	1520.4	30.18	0.549	67	0	0
IV	155.1	80.5	356.8	592.4	7.59	0.152	0	0	33
V	124.4	64.6	326.7	515.7	6.95	0.133	18	53	17
VI	138.4	71.8	314.7	524.9	6.70	0.128	10	50	22
VII	139.8	72.6	341.8	554.2	7.27	0.136	67	61	9
VIII	649.6	337.1	222.3	1209	4.73	0.086	0	0	138

Table 9
Simulated results of the proposed approach and Ref. [26].

Approach	Numbers			SAIDI [h/yr.LP]	Execution time
	FI	MS	RCS		
Proposed approach	18	53	17	0.133	55.64 s
[26]	14	37	16	0.137	2.51 h

same preset conditions, and three cases are considered for comparison. The crossover rate and mutation rate are determined to be 0.8 and 0.05. The results between the proposed MIP model and GA are shown in Table 5.

Case A: solving the proposed model in the MIP method;

Case B: solving the proposed model via GA. The population size and maximum generations are determined to be 24 and 100;

Case C: solving the proposed model via GA. The population size and maximum generations are determined to be 50 and 400.

Table 5 shows that the total cost in the MIP method is less than that provided by GA. The run time of Case B is less than that of Case C but with a worse solution. The proposed method can obtain the global optimal solution after converting the FI and SS placement problem into an MIP model, preventing operators' experience and the adopted parameters from influencing the results of GA [32]. Moreover, the computational speed of the proposed method is much faster than that of GA.

4.1.2. Sequential placement

Conventionally, the SS and FI allocation problem is addressed in a sequential manner wherein the SS allocation problem is first considered, and then the FIs allocation is performed [26]. In the SSs placement of Case VI above, the fault location time relies on the deployment of the RCSs. In the practical SS allocation problem, the exact fault location time is unknown because the FIs could influence the fault location procedure, and the placement of them is not determined. Therefore, planners will adopt an expected fault location time that is guessed based on engineering experience. To this end, several expected fault location times are adopted in the sequential placement problem, and the results are shown in Table 6.

According to the results shown in Table 6, different expected fault location times will lead to changes in the location and number of SSs. Further, the allocation of the FIs changes following the placement of the SSs. Therefore, the sequential placement of SSs and FIs cannot obtain the exact and precise solution. However, the accurate fault location time can be achieved by considering RCSs and FIs simultaneously.

4.1.3. Unit interruption cost

Clearly, the unit interruption cost plays a major role in the optimization problem. The willingness of electric utilities to increase the service reliability depends on the outage cost. To investigate the impact of the unit interruption cost on the deployment problem, several e_{unit} values are adopted, and the results are shown in Table 7.

The total number of FIs and SSs increases as the unit interruption cost increases. The number of deployed RCSs is less than that of MSs because the RCS is more expensive. Therefore, when the budget is limited, electric utilities can improve the reliability by equipping more FIs and MSs.

4.1.4. The number of installed equipment

The numbers of FIs and SSs allowed to be placed would influence the solution of the FI and SS placement problem. Fig. 3 shows the variations in the SAIDI, the equipment-related cost that includes the capital and maintenance costs of the equipment, and the total costs versus the number of installed equipment.

By increasing the numbers of FIs and SSs, the total costs are first reduced and then increased again. Hence, installing more FIs and SSs is not always beneficial. The variations in the SAIDI and equipment-related costs are opposite, as a higher investment in equipment results in a more reliable power supply.

4.2. Finnish 20 kV urban distribution system

An example of a practical medium voltage distribution system is given to illustrate the efficiency and effectiveness of the proposed

model in large networks. There are 6 interconnected feeders and 144 load points in the system; data can be found in Ref. [3]. Eight different cases, the same as the cases adopted for IEEE 33-bus, are simulated. The resultant costs, reliability indices and equipment deployment results of Cases I–VIII are presented in Table 8. The execution times associated with the allocation results of the proposed approach and Ref. [26] are presented in Table 9.

In Table 8, Case V has the most optimum solution. The equipment cost of Case IV is higher than that of Case V, but the reliability indices of Case IV are worse than those of Case V. Thus, although the performance of the RCS is better than MS and FI, it is unable to obtain a more economical and efficient solution by configuring RCSs separately. The reliability indices of Case VI are superior to those of Case V; however, Case V is economically optimal for electric utilities. Hence, the simultaneous placement of FIs and SSs in distribution networks can achieve significant reductions in costs and outage durations with a lower investment cost. Table 9 shows that the execution time of the proposed approach for this large-scale distribution network is still efficient, even though the run time of Ref. [26] can be reduced to 10 min when the optimal gap is set to 0.5%. The proposed three position matrices summary the pathway and customer information of the distribution networks, thereby simplifying the constraints associated with fault location and fault isolation and narrowing the search space of the placement problem.

5. Conclusions

This paper simultaneously establishes a model for the optimal placement of FIs and SSs in complex distribution networks. To obtain a more precise reliability evaluation, the customer interruption duration under different contingencies is formulated and built as a function of the FI, RCS and MS locations. Additionally, three position matrices are derived and used to construct the customer outage time. The relevant results show that (i) simultaneously considering the placement of FIs and SSs can speed up the fault location and isolation process, thereby reducing the customer interruption duration; (ii) the proposed model can reduce costs and improve the system quality of service significantly to achieve the best balance between the reliability investment and the reliability benefit; and (iii) the proposed method is superior to the GA and has a high computational efficiency.

Declaration of Competing Interest

The authors declare that they have no known competing financial interests or personal relationships that could have appeared to influence the work reported in this paper.

Acknowledgments

This work was supported by the National Natural Science Foundation of China (51307063) and the Key Science and Technology Project of China Southern Power Grid Co., Ltd. (090000KK52180116).

References

[1] A. Heidari, V.G. Agelidis, M. Kia, J. Pou, J. Aghaei, M. Shafie-Khah, J.P.S. Catalao, Reliability optimization of automated distribution networks with probability customer interruption cost model in the presence of DG units, IEEE Trans. Smart Grid 8 (1) (2017) 305–315.
[2] Y. He, Modelling and Evaluating Effect of Automation, Protection, and Control on Reliability of Power Distribution Systems (Ph.D. Dissertation), Royal Inst. Technol., KTH Royal Institute of Technology, 2002.
[3] S. Kazemi, Reliability Evaluation of Smart Distribution Grids (Ph.D. Dissertation), Depts. Elec. Eng., Sharif University of Technology and Aalto University, 2011.
[4] J.A. Momoh, Electric Power Distribution, Automation, Protection, and Control, CRC Press, 2007.
[5] C.Y. Ho, T.E. Lee, C.H. Lin, Optimal placement of fault indicators using the immune algorithm, IEEE Trans. Power Syst. 26 (1) (2011) 38–45.
[6] H. Falaghi, M.R. Haghifam, C. Singh, Ant colony optimization-based method for placement of sectionalizing switches in distribution networks using a fuzzy multi-objective approach, IEEE Trans. Power Deliv. 24 (1) (2009) 268–276.
[7] G. Levitin, S. Mazal-Tov, D. Elmakis, Optimal sectionalizer allocation in electric distribution systems by genetic algorithm, Electr. Power Syst. Res. 31 (1994) 97–102.
[8] R. Billinton, S. Jonnavithula, Optimal switching device placement in radial distribution system, IEEE Trans. Power Deliv. 11 (3) (1996) 1646–1651.
[9] L.S. De Assis, J.F.V. Gonzalez, F.L. Usberti, C. Lyra, C. Cavellucci, F.J. Von Zuben, Switch allocation problems in power distribution systems, IEEE Trans. Power Syst. 30 (1) (2014) 246–253.
[10] Y. Xu, C.C. Liu, K.P. Schneider, D.T. Ton, Placement of remote-controlled switches to enhance distribution system restoration capability, IEEE Trans. Power Syst. 31 (2) (2016) 1139–1150.
[11] C.S. Chen, C.H. Lin, H.J. Chuang, C.S. Li, M.Y. Huang, C.W. Huang, Optimal placement of line switches for distribution automation systems using immune algorithm, IEEE Trans. Power Syst. 21 (3) (2006) 1209–1217.
[12] J.R. Bezerra, G.C. Barroso, R.P.S. Leao, R.F. Sampaio, Multiobjective optimization algorithm for switch placement in radial power distribution networks, IEEE Trans. Power Deliv. 30 (2) (2015) 545–552.
[13] P.M.S. Carvalho, L.A.F.M. Ferreira, A.J.C. Da Silva, A decomposition approach to optimal remote controlled switch allocation in distribution systems, IEEE Trans. Power Deliv. 20 (2) (2005) 1031–1036.
[14] O.K. Siirto, A. Safdarian, M. Lehtonen, M. Fotuhi-Firuzabad, Optimal distribution network automation considering earth fault events, IEEE Trans. Smart Grid 6 (2) (2017) 1010–1018.
[15] J.C. López, J.F. Franco, M.J. Rider, Optimization-based switch allocation to improve energy losses and service restoration in radial electrical distribution systems, IET Gener. Transm. Distrib. 10 (11) (2016) 2792–2801.
[16] M. Farajollahi, M. Fotuhi-Firuzabad, A. Safdarian, Optimal placement of sectionalizing switch considering switch malfunction probability, IEEE Trans. Smart Grid 10 (1) (2019) 403–413.
[17] A. Shahsavari, A. Fereidunian, S.M. Mazhari, A joint automatic and manual switch placement within distribution systems considering operational probabilities of control sequences, Int. Trans. Electr. Energy Syst. 25 (2015) 2745–2768.
[18] R. Dashti, J. Sadeh, Fault indicator allocation in power distribution network for improving reliability and fault section estimation, 2011 Int. Conf. Adv. Power Syst. Autom. Prot. (2011) 1406–1411.
[19] W.F. Usida, D.V. Coury, R.A. Flauzino, I.N. da Silva, Efficient placement of fault indicators in an actual distribution system using evolutionary computing, IEEE Trans. Power Syst. 27 (4) (2012) 1841–1849.
[20] D.P. Cong, B. Raison, J.P. Rognon, S. Bonnoit, B. Manjal, Optimization of fault indicators placement with dispersed generation insertion, IEEE Power Engineering Society General Meeting (2005) 355–362.
[21] A. Shahsavari, S.M. Mazhari, A. Fereidunian, H. Lesani, Fault indicator deployment in distribution systems considering available control and protection devices: a multi-objective formulation approach, IEEE Trans. Power Syst. 29 (5) (2014) 2359–2369.
[22] R.B. Hendi, S.J. Seyed-Sheneva, M. Gandomkar, Electrical distribution system reliability improvement by optimal placement of fault indicators using immune algorithm, Int. J. Eng. Res. Appl. 2 (2012) 1383–1390.
[23] J.H. Teng, W.H. Huang, S.W. Luan, Automatic and fast faulted line-section location method for distribution systems based on fault indicators, IEEE Trans. Power Syst. 29 (4) (2014) 1653–1662.
[24] M. Farajollahi, M. Fotuhi-Firuzabad, A. Safdarian, Deployment of fault indicator in distribution networks: a MIP-based approach, IEEE Trans. Smart Grid 9 (3) (2018) 2259–2267.
[25] M.H. Kapourchali, M. Sepehry, V. Aravinthan, Fault detector and switch placement in cyber-enabled power distribution network, IEEE Trans. Smart Grid 9 (2) (2018) 980–992.
[26] M. Farajollahi, M. Fotuhi-Firuzabad, A. Safdarian, Simultaneous placement of fault indicator and sectionalizing switch in distribution networks, IEEE Trans. Smart Grid 10 (2) (2019) 2278–2287.
[27] H.L. Willis, Power Distribution Planning Reference Book, 2nd edn., Marc Dekker, Inc., New York, 2004.
[28] R. Billinton, W. Wangdee, Approximate methods for event-based customer interruption cost evaluation, IEEE Trans. Power Syst. 20 (2) (2005) 1103–1110.
[29] IBM ILOG CPLEX, (2017) [Online]. Available: http://www-01.ibm.com/software/commerce/optimization/cplex-optimizer.
[30] R. Billinton, J. Billinton, Distribution system reliability indices, IEEE Trans. Power Deliv. 4 (1) (1989) 561–568.
[31] M.E. Baran, F.F. Wu, Network reconfiguration in distribution systems for loss reduction and load balancing, IEEE Trans. Power Deliv. 4 (2) (1989) 1401–1407.
[32] K.Y. Lee, M.A. El-Sharkawi, Modern Heuristic Optimization Techniques: Theory and Applications to Power Systems, Wiley, Hoboken, NJ, USA, 2008.